

Heliospheric Plasma Sheet (HPS) Impingement onto the Magnetosphere as a Cause of Relativistic Electron Dropouts (REDs) via Coherent EMIC Wave Scattering with Possible Consequences for Climate Change Mechanisms

B.T. Tsurutani¹, R. Hajra², T. Tanimori³, A. Takada³, B. Remya⁴, A.J. Mannucci¹, G.S.
Lakhina⁵, J.U. Kozyra⁶, K. Shiokawa⁷, L.C. Lee⁴, E. Echer², R.V. Reddy⁴, and W.D.
Gonzalez²

¹Jet Propulsion Laboratory, California Institute of Technology, Pasadena, CA

²Instituto Nacional de Pesquisas Espaciais, Sao Jose dos Campos, SP, Brazil

³Faculty of Science, Kyoto University, Sakyo-ku, Kyoto 6068502, Japan

⁴Academia Sinica, Taipei, Taiwan

⁵Indian Institute of Geomagnetism, Navi Mumbai, India

⁶National Science Foundation, Wash. D.C.

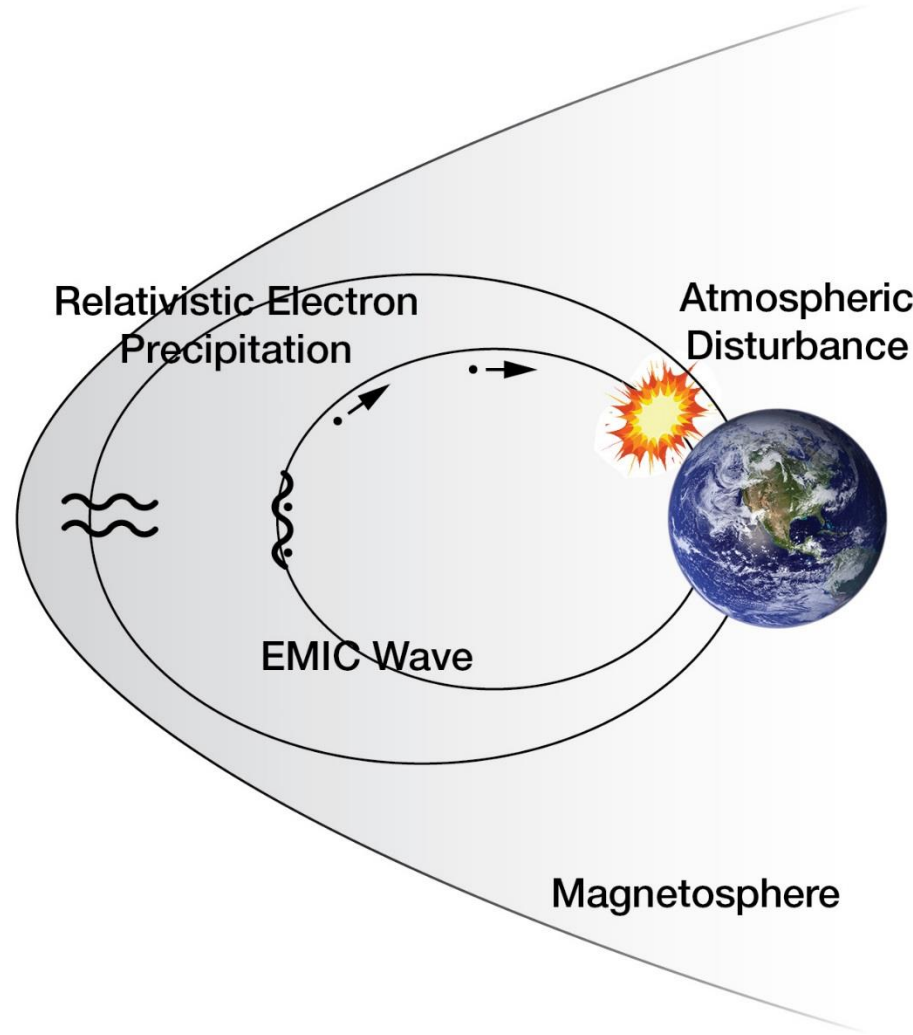
⁷Institute for Space Earth Environmental Research, Nagoya University, Nagoya, Japan

JGRSP, 121, doi:10.1002/2016JA022499, 2016

Questions/Comments to: Bruce.Tsurutani@jpl.nasa.gov



Heliospheric Plasma Sheet
(HPS)



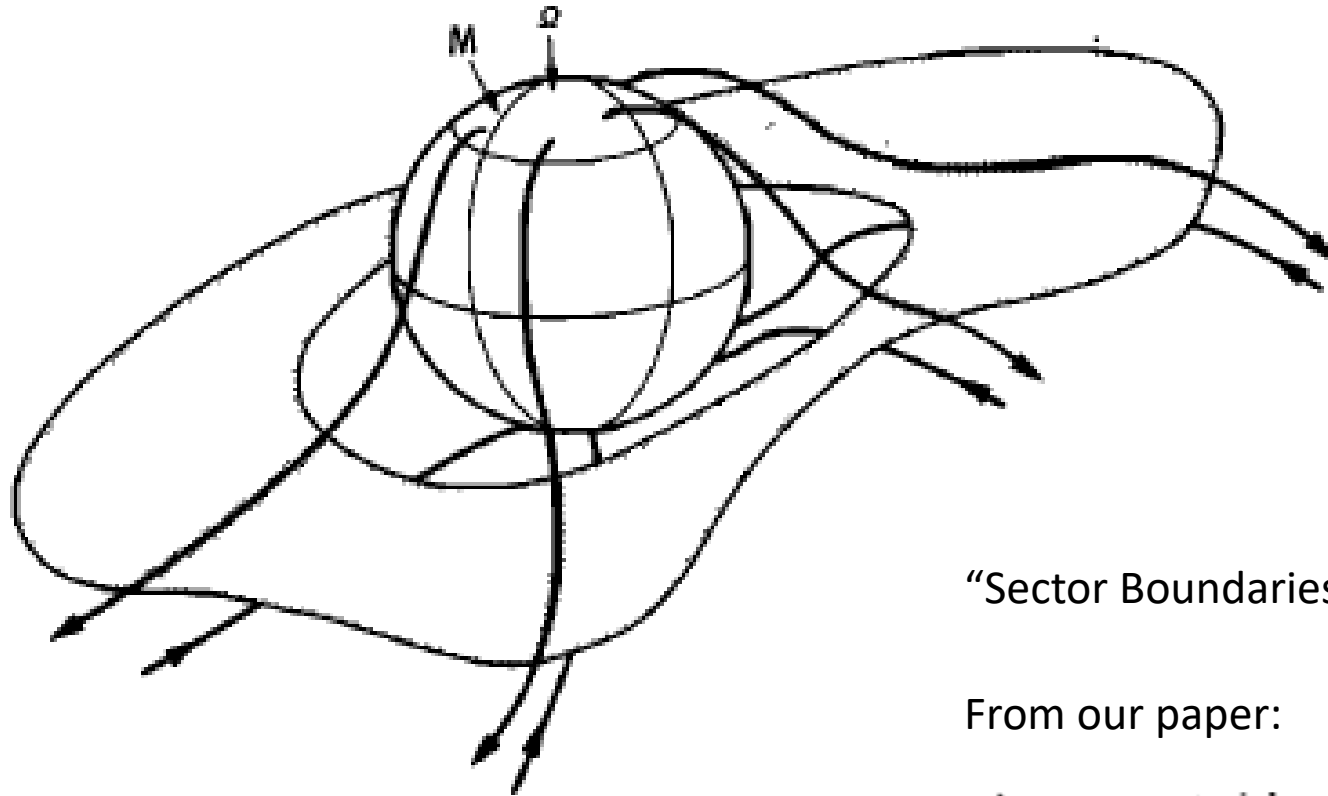
Relativistic Electron
Precipitation

Atmospheric
Disturbance

EMIC Wave

Magnetosphere

Abstract A new scenario is presented for the cause of magnetospheric relativistic electron decreases (REDs) and potential effects in the atmosphere and on climate. High-density solar wind heliospheric plasmashet (HPS) events impinge onto the magnetosphere, compressing it along with remnant noon-sector outer-zone magnetospheric $\sim 10\text{-}100$ keV protons. The betatron accelerated protons generate coherent electromagnetic ion cyclotron (EMIC) waves through a temperature anisotropy ($T_{\perp}/T_{\parallel} > 1$) instability. The waves in turn interact with relativistic electrons and cause the rapid loss of these particles to a small region of the atmosphere. A peak total energy deposition of $\sim 3 \times 10^{20}$ ergs is derived for the precipitating electrons. Maximum energy deposition and creation of electron-ion pairs at 30-50 km and at < 30 km altitude are quantified. We focus the readers' attention on the relevance of this present work to two climate change mechanisms. Wilcox et al. (1973) noted a correlation between solar wind heliospheric current sheet (HCS) crossings and high atmospheric vorticity centers at 300 mb altitude. Tinsley et al. (1994) has constructed a global circuit model which depends on particle precipitation into the atmosphere. Other possible scenarios potentially affecting weather/climate change are also discussed.

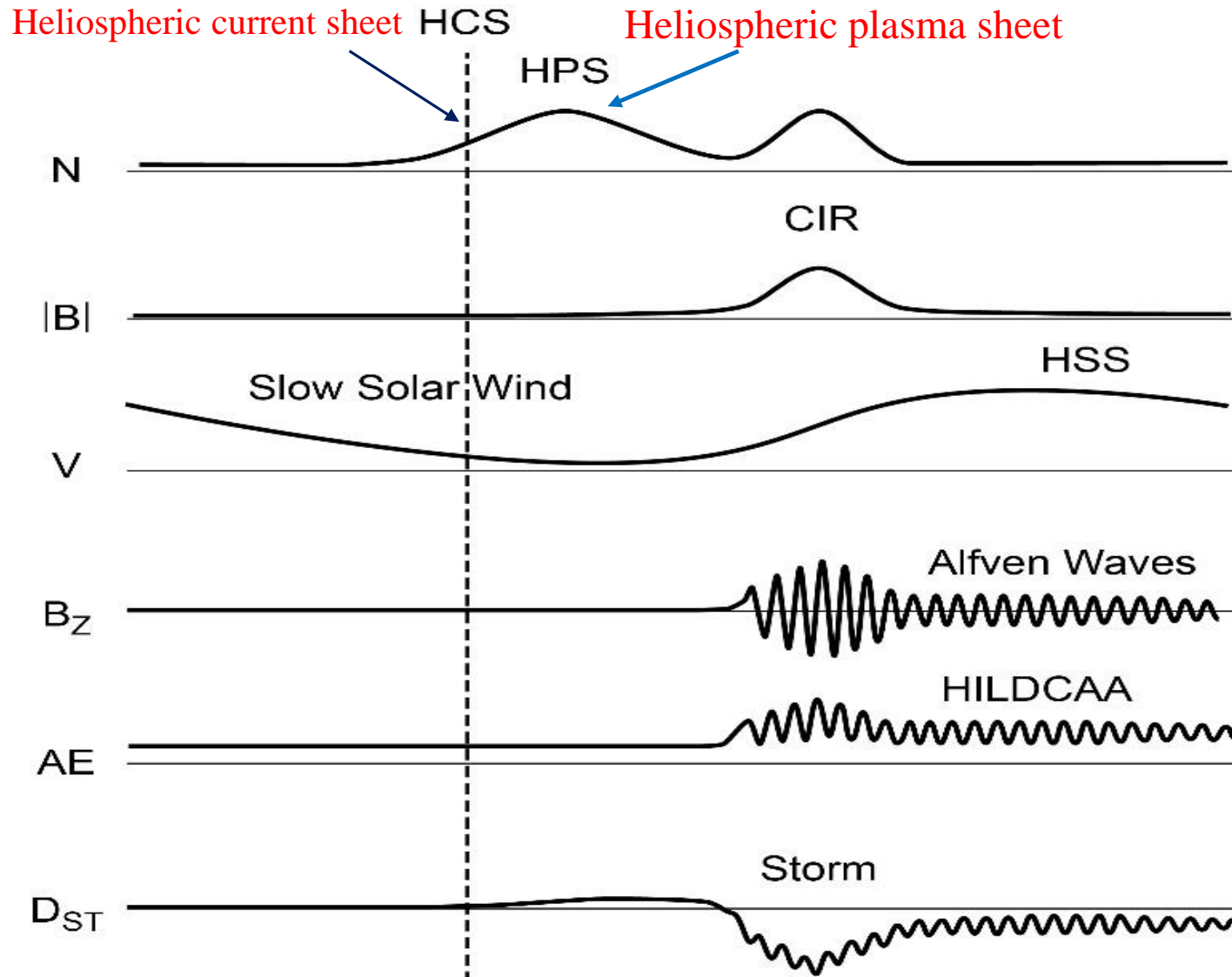


“Sector Boundaries”: Ness and Wilcox, PRL 1964

From our paper:

A near-equatorial current sheet has also been advocated. When the four-sector structure was first observed, H. Alfvén (personal communication, 1965) immediately interpreted it in terms of successive penetrations of a current sheet encircling the sun and lying near the solar equator but distorted or warped somewhat by flutes or folds. Following the discovery

Discovery of the HCS by the Pioneer 11 magnetometer team
(Smith, Tsurutani, Rosenberg, JGR 1978)



HPS occurs before CIR and HSS

Selection of Low Speed and High Speed Solar Wind Intervals **Without Magnetic Storms**: 8 Events in SC23

#	Event	Start (DOY UT)	End (DOY UT)	Duration (h)	Peak pressure (nPa)	HCS time (DOY UT)
1	1995_150	150 02:39	150 05:37	3.0	26.6	150 04:44
2	1998_202	202 02:38	202 06:45	4.1	18.6	202 04:27
3	2000_027	027 14:04	027 21:35	7.5	20.3	027 18:03
4	2000_052	052 01:11	052 08:13	7.0	14.8	----
5	2003_258	258 16:32	259 03:16	10.7	8.0	258 20:43
6	2007_056	056 12:00	057 05:32	17.3	12.2	057 03:21
7	2007_243	243 13:43	243 20:52	7.2	5.1	243 21:37
8	2008_058	058 14:07	058 19:48	5.7	9.6	058 17:51

Relativistic Electron Decreases (REDs)

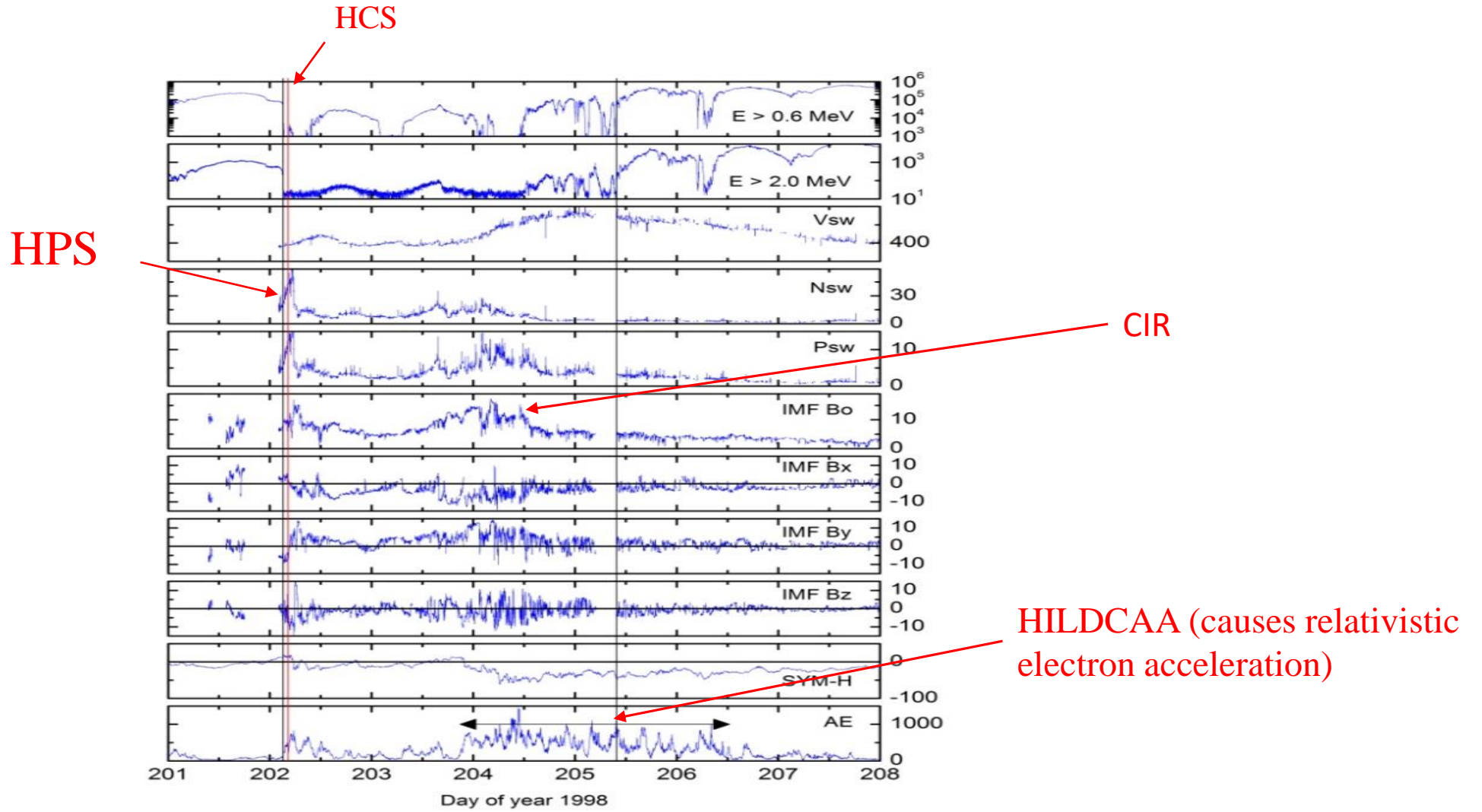


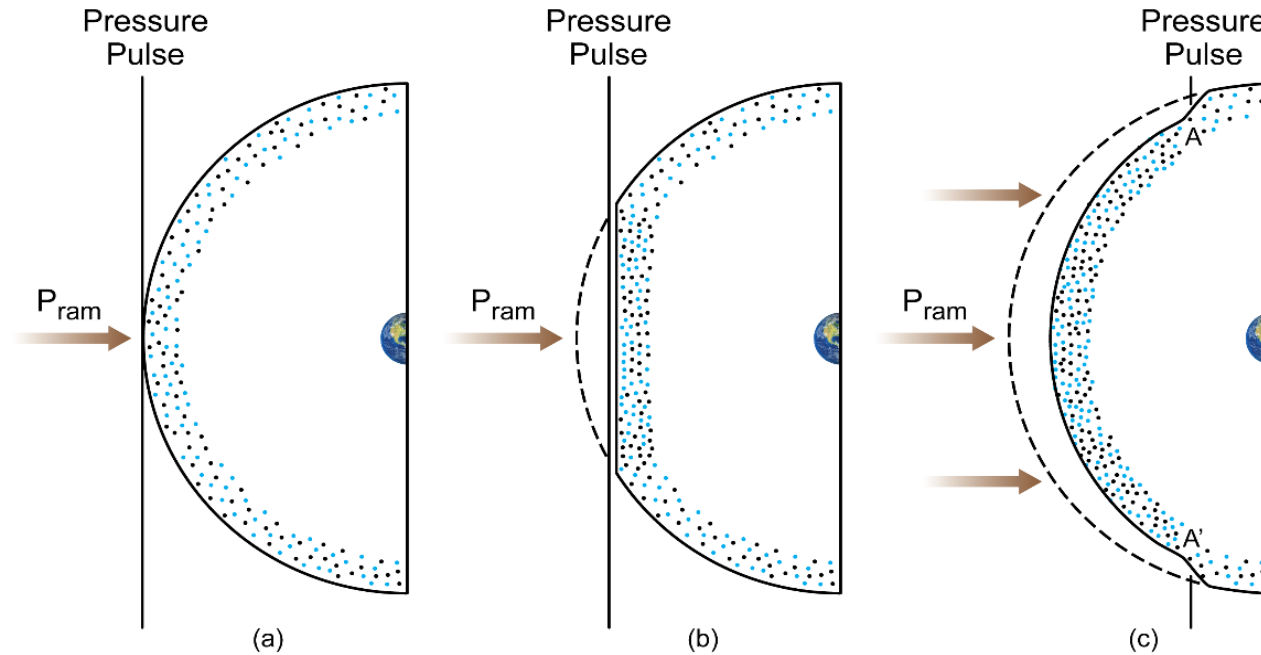
Table 1. Eight HPS Pressure Pulse Events From SC23 That Were Not Followed by Magnetic Storms^a

Number	Event	Start (DOY UT)	End (DOY UT)	Duration (h)	Peak Pressure (nPa)	HCS Time (DOY UT)
1	1995_150	150 02:39	150 05:37	3.0	26.6	150 04:44
2	1998_202	202 02:38	202 06:45	4.1	18.6	202 04:27
3	2000_027	027 14:04	027 21:35	7.5	20.3	027 18:03
4	2000_052	052 01:11	052 08:13	7.0	14.8	—
5	2003_258	258 16:32	259 03:16	10.7	8.0	258 20:43
6	2007_056	056 12:00	057 05:32	17.3	12.2	057 03:21
7	2007_243	243 13:43	243 20:52	7.2	5.1	243 21:37
8	2008_058	058 14:07	058 19:48	5.7	9.6	058 17:51

^aAll eight HPS impacts on the magnetosphere were associated with REDs.

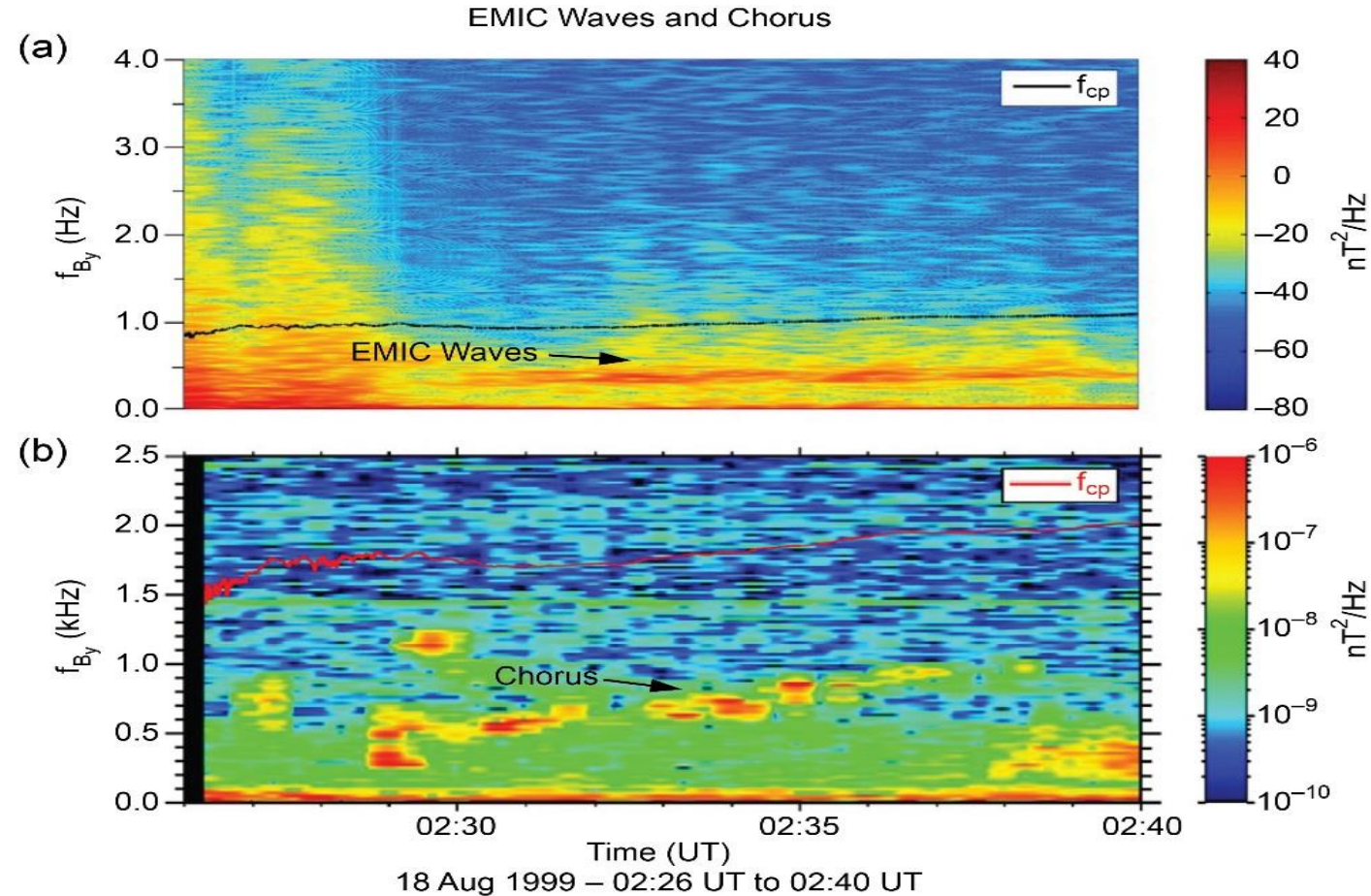
All 8 intervals had RED events. All events were caused by HPS impingements onto the magnetosphere. The typical RED decay time ~ 1 hr

The Solar Wind HPS Will Compress the Dayside Magnetosphere

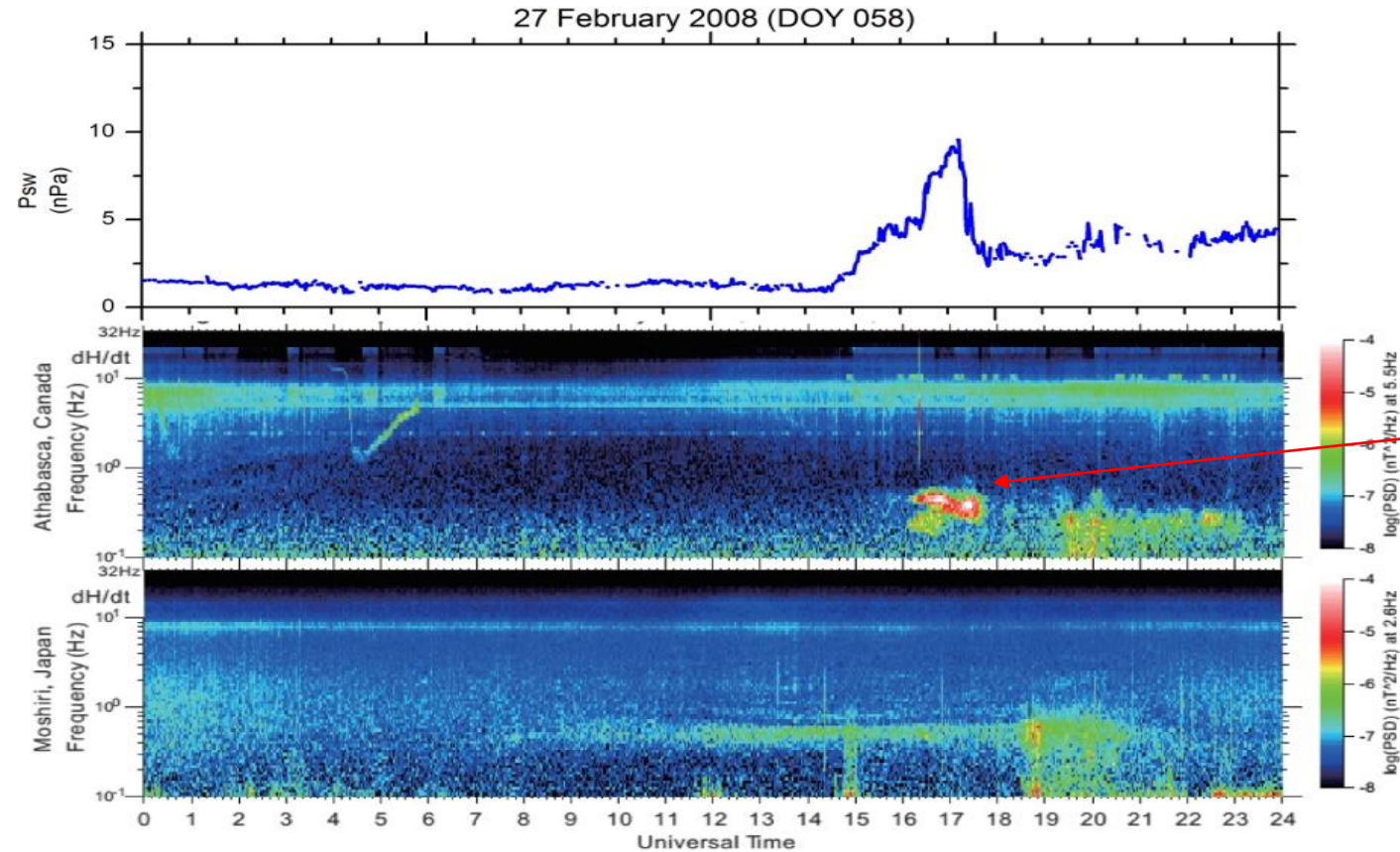


The solar wind pressure pulse will cause the **betatron acceleration of preexisting $\sim 10-100$ keV electrons and protons in T_{\perp} and thus instability** in both particles.

Simultaneous EMIC and Chorus Waves from L = 10 to 7 at ~1300 MLT Cassini Near-Earth Swing-By During a Solar Wind Pressure Pulse



Simultaneous HPS Impingement and Nagoya Univ. ISEE Ground Magnetometer EMIC Waves

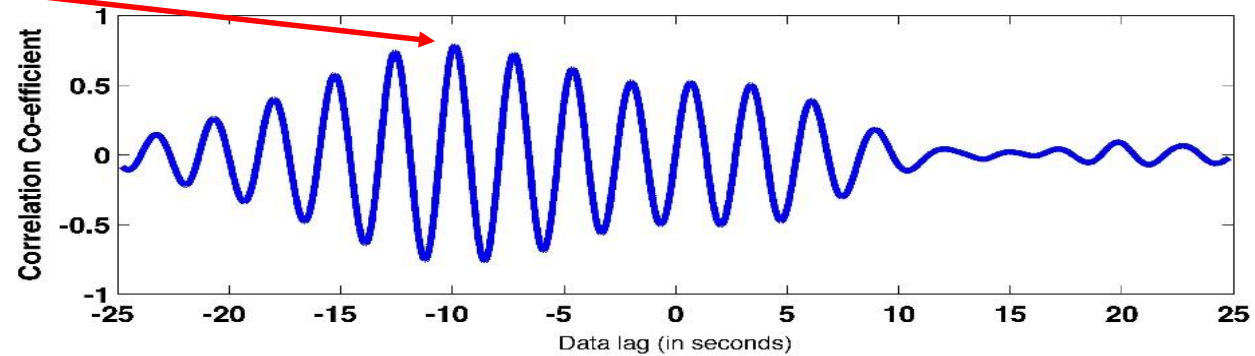
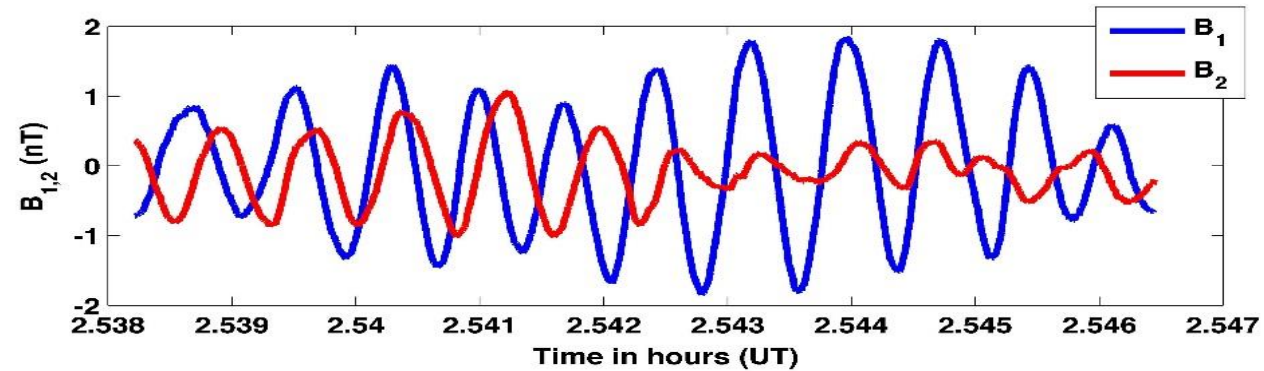


Athabasca, Canada
61.7° MLAT, ~09 MLT

Moshiri, Japan
35° MLAT, ~02 MLT

What Do the EMIC Waves Look Like in Detail?

EMIC waves
are “coherent”



With coherent waves, the pitch angle transport of resonant particles will be
3 orders of magnitude larger than standard theory.



Pitch angle scattering of an energetic magnetized particle by a circularly polarized electromagnetic wave

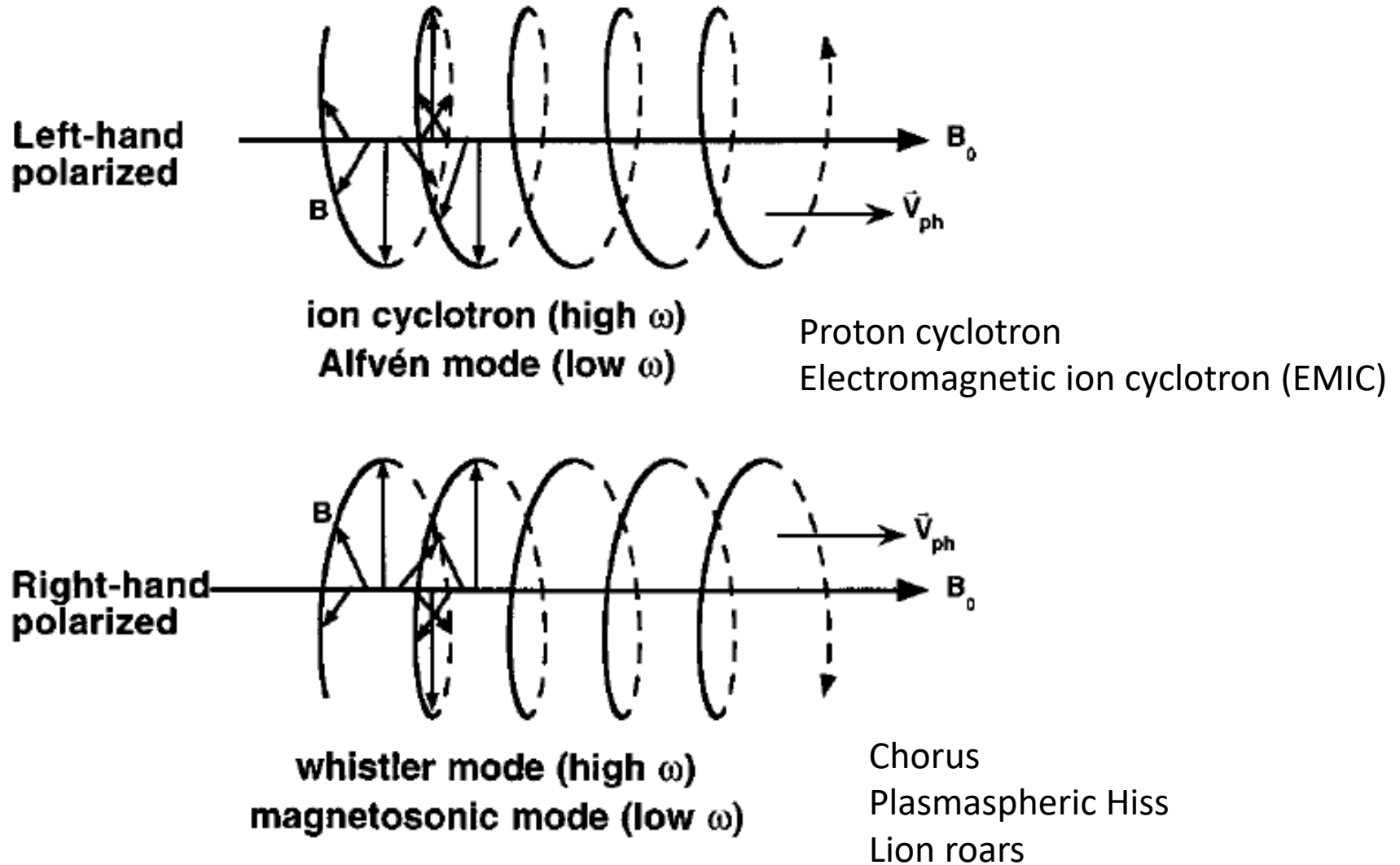
P. M. Bellan

Applied Physics, Caltech, Pasadena, California 91125, USA

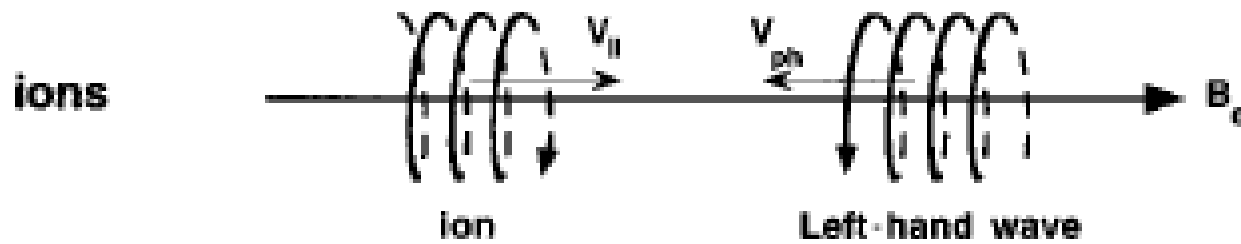
(Received 7 February 2013; accepted 26 March 2013; published online 19 April 2013)

The interaction between a circularly polarized wave and an energetic gyrating particle is described using a relativistic pseudo-potential that is a function of the frequency mismatch. Analysis of the pseudo-potential provides a means for interpreting numerical results. The pseudo-potential profile depends on the initial mismatch, the normalized wave amplitude, and the initial angle between the wave magnetic field and the particle perpendicular velocity. For zero initial mismatch, the pseudo-potential consists of only one valley, but for finite mismatch, there can be two valleys separated by a hill. A large pitch angle scattering of the energetic electron can occur in the two-valley situation but fast scattering can also occur in a single valley. **Examples relevant to magnetospheric whistler waves show that the energetic electron pitch angle can be deflected 5° towards the loss cone when transiting a 10 ms long coherent wave packet having realistic parameters.** © 2013 AIP Publishing LLC [<http://dx.doi.org/10.1063/1.4801055>]

Electromagnetic Wave Polarizations



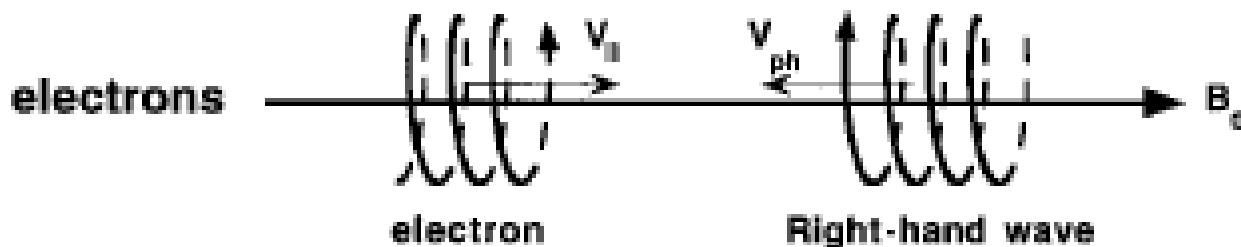
(Normal) Cyclotron Resonance



$$\omega - \bar{\mathbf{k}} \cdot \bar{\mathbf{V}} = \Omega^+$$

$$\omega + k_{||} V_{||} = \Omega^+$$

The relative motion between the wave and particle Doppler shifts the wave up to the ion cyclotron frequency.



$$\omega + k_{||} V_{||} = \Omega^-$$

EMIC Waves Cyclotron Resonant with 0.6 to 0.9 MeV Electrons

Table 3. Electron Anomalous Cyclotron Resonance With Two Cycles of an EMIC Wave of Conservative Amplitude 2.0 nT at a Variety of Different L Shells^a

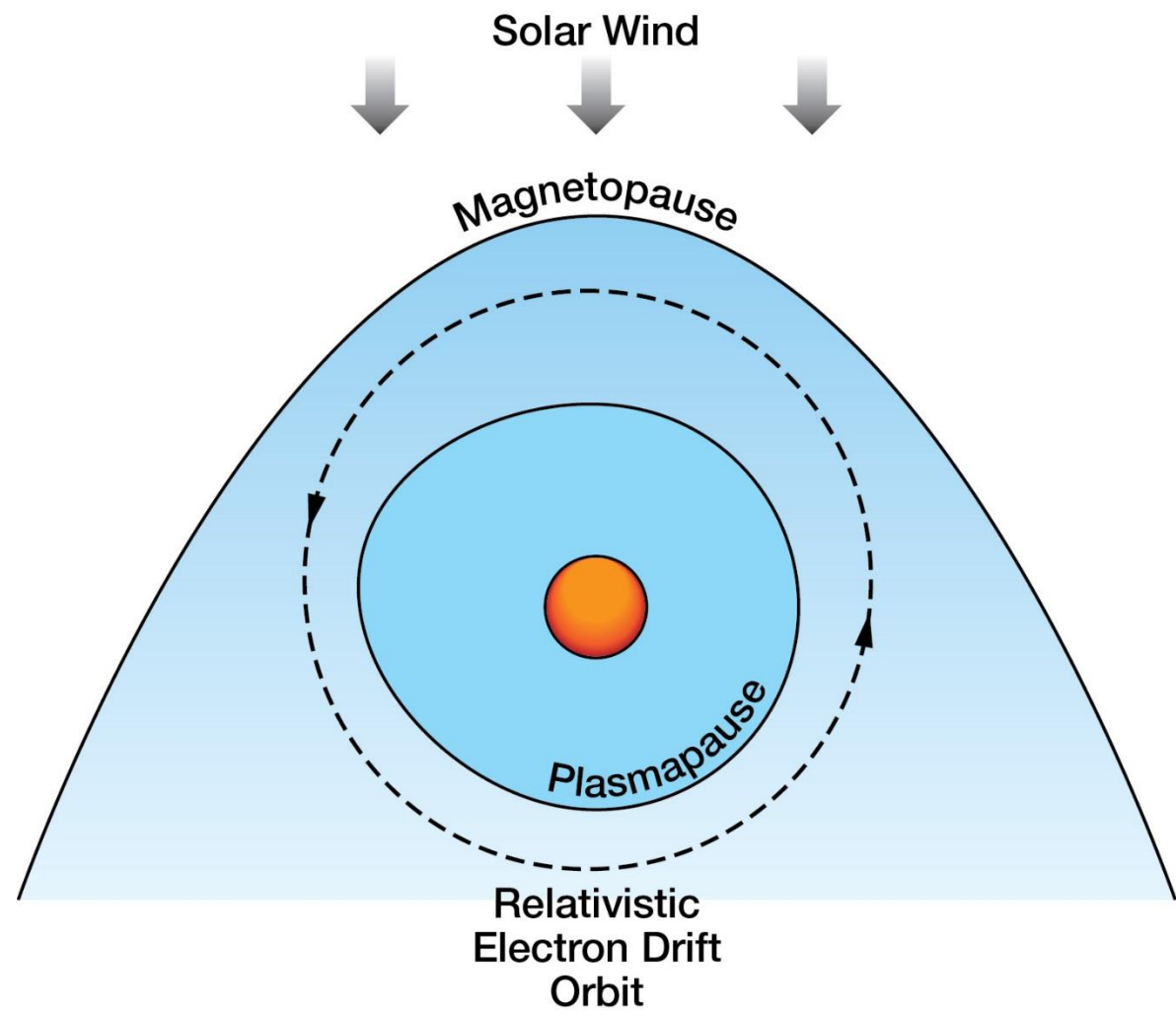
Parameters	L = 10	L = 9	L = 8	L = 7	L = 6
V_{ph} (* 10 ⁵ m/s)	2.2643	2.1946	2.3163	2.3732	3.499
Ω_e (* 10 ⁴ rad/s)	1.077	1.0873	1.2956	1.4756	3.4274
ω (rad/s)	3.107	2.255	2.6	3	3
$V_{ }$ (* 10 ⁸ m/s)	2.8025	2.886	2.9037	2.9057	2.9916
γ	2.8	3.66	3.98	4.019	13.37
$E_{ }$ (MeV)	0.625	0.87	0.954	0.964	3.4
Δt (ms)	4.357	4.11	4.37	4.41	6.32
$\Delta\alpha$ (deg)	31.5	22.6	22.2	22.1	9.5
D (s ⁻¹)	34.65	18.87	17.08	16.85	2.18
T (ms)	28.9	53	58.5	59.3	457.8

^aThe rows, from top to bottom, are the wave phase velocity, the electron cyclotron frequency at the equator, the parallel speed of the electron along B_0 , the parallel kinetic energy of the electron, the time of wave-particle interaction, the amount of particle pitch angle transport, the diffusion coefficient D , and the time for particle pitch angle diffusion T .

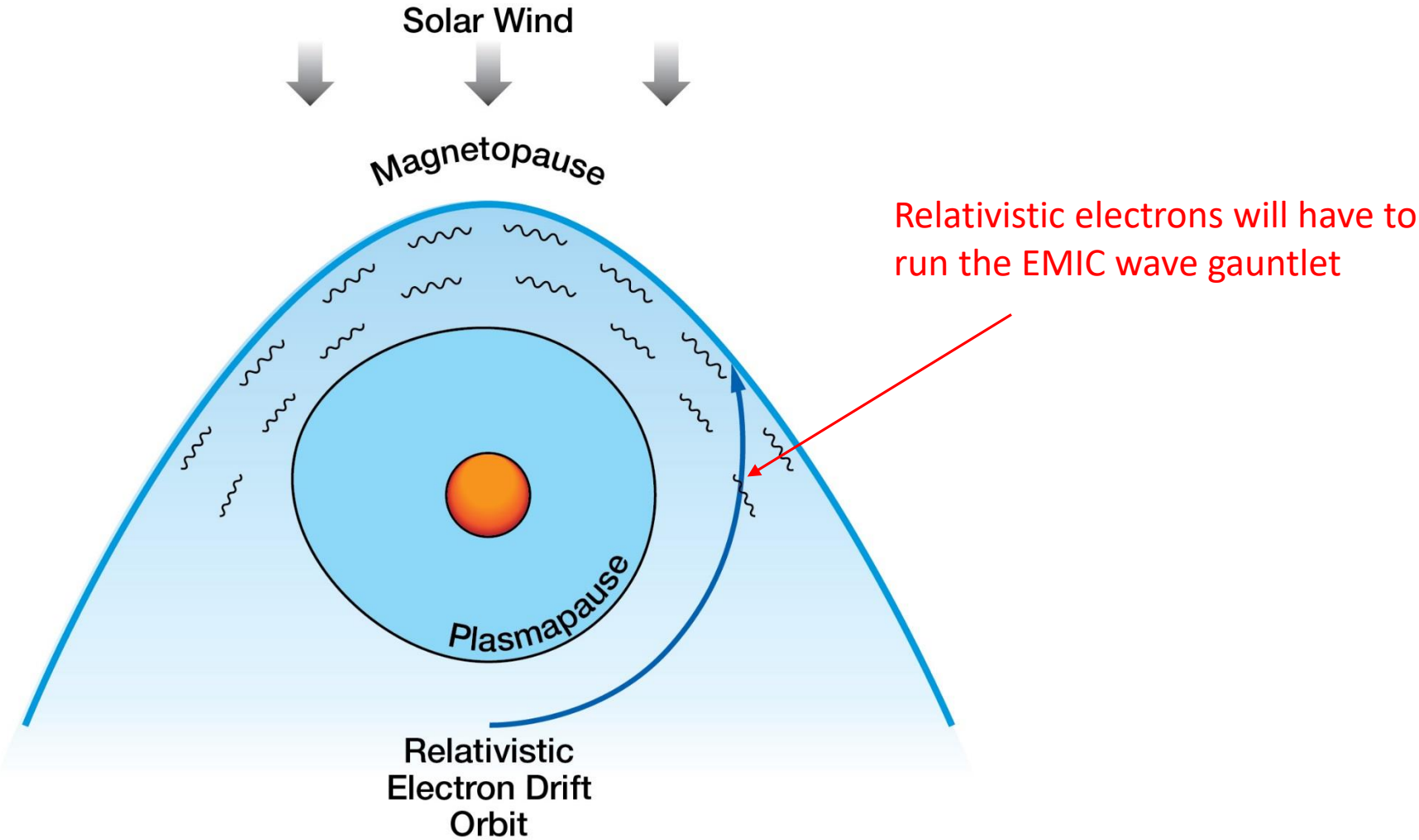
The change $\Delta\alpha$ in particle pitch angle for arbitrary α is obtained as: $\Delta\alpha = \frac{B}{B_0} \Omega \Delta t$

$$\Delta\alpha = 23^\circ; T = 53 \text{ ms}$$

“Before”

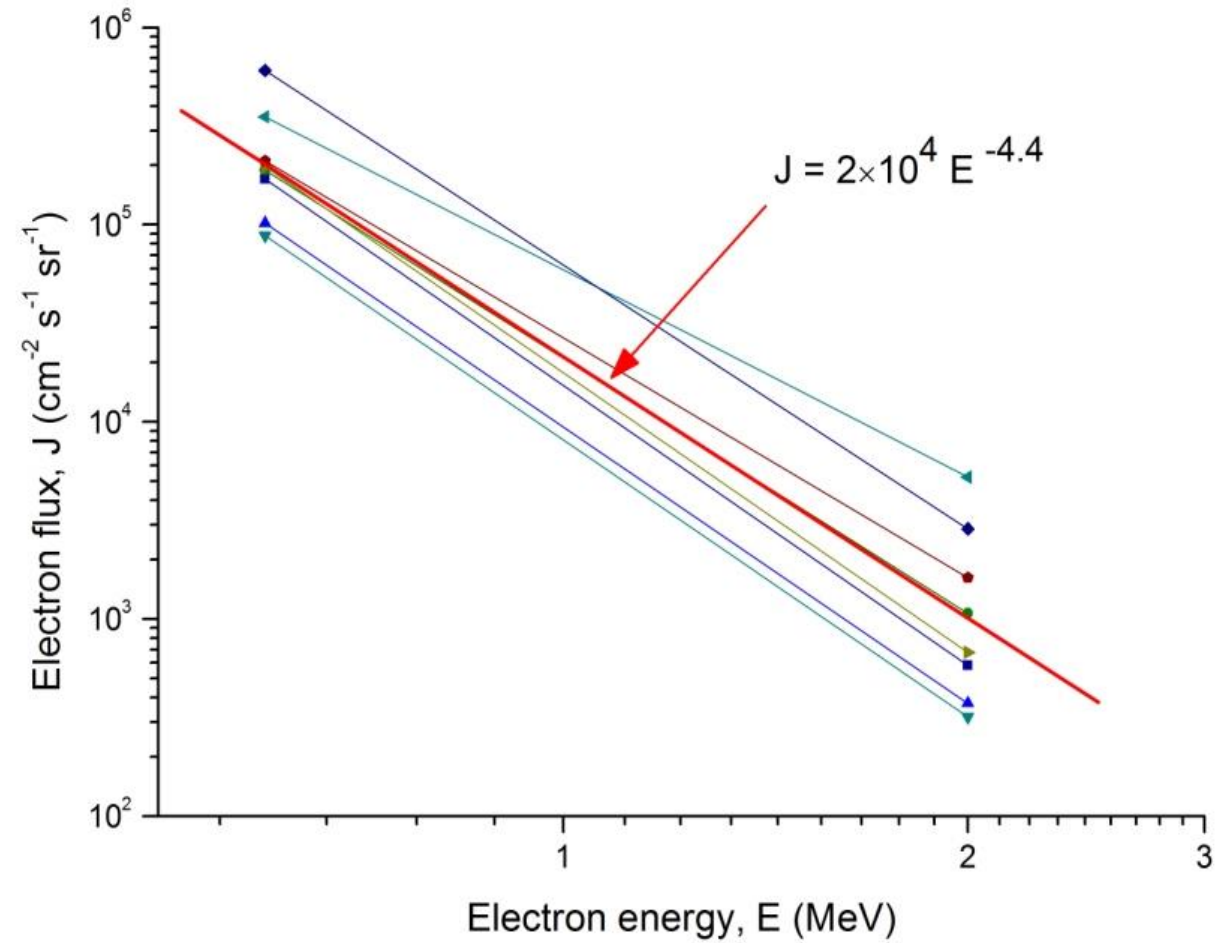


“After”



Relativistic electrons will have to run the EMIC wave gauntlet

2-Point Power Spectra for the Eight Events



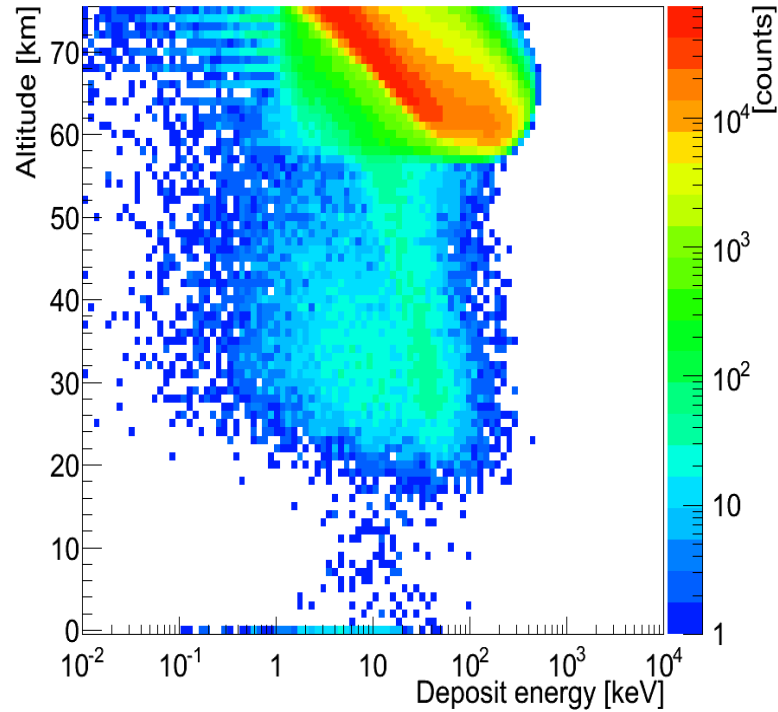
Total Magnetospheric Particle Energy Calculations

A flux decrease of $\sim 10^5$ particles $\text{cm}^{-2} \text{s}^{-1} \text{ster}^{-1}$ in the $E > 0.6$ MeV energy range (~ 1 MeV electrons) was determined from measurements.

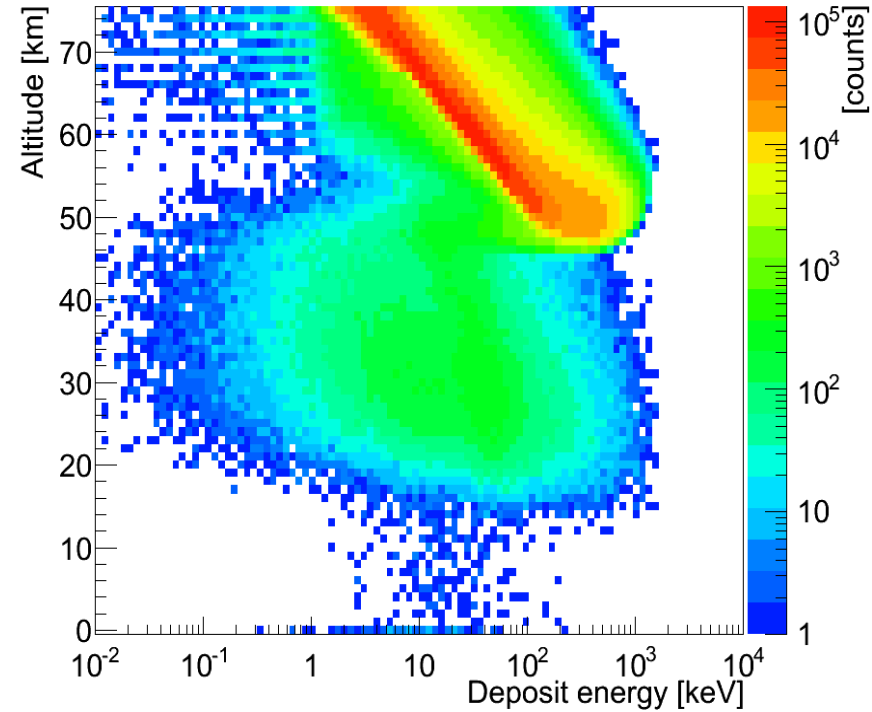
The bounce time of a charged particle is $T_B = L R_E (3.7 - 1.6 \sin \alpha) V_e$ (Baumjohann and Treumann, 2012). Assuming a 2π ster downward flux and a constant flux from $L = 6$ to 10,

The total energy of ~ 1 MeV electrons in the magnetosphere from $L = 6$ to 10 is $\sim 3 \times 10^{20}$ ergs.

The GEANT4 Monte Carlo Code Developed by CERN



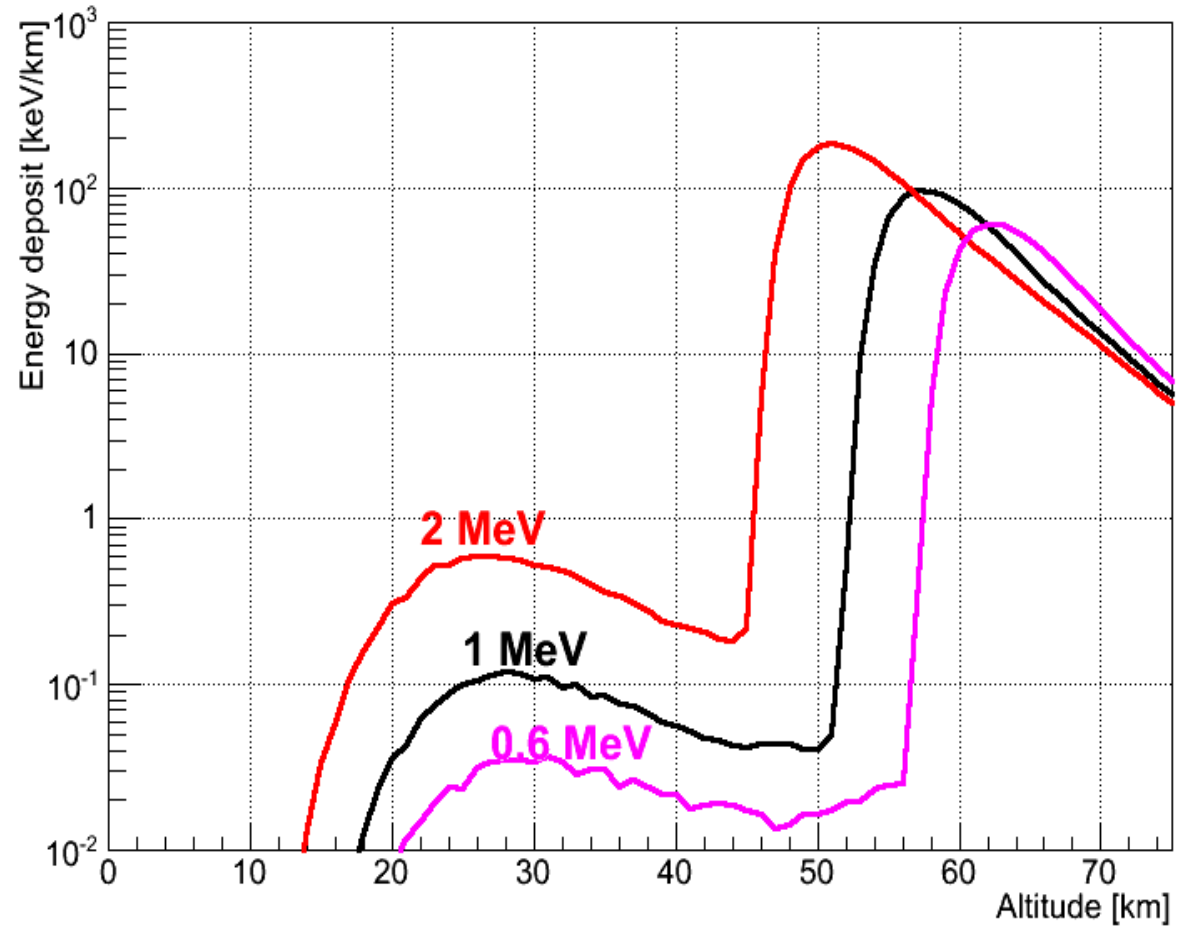
$E = 0.6 \text{ MeV}$



$E = 2.0 \text{ MeV}$

Vertical magnetic fields assumed in simulations

Energy Deposition as Function of Initial Energy and Altitude



For $E > 0.6 \text{ MeV}$ electrons a maximum of $\sim 4 \times 10^{17}$ ergs deposited between 50 and 30 km and $\sim 3.0 \times 10^{17}$ ergs deposited below 30 km altitude

For $E > 2.0 \text{ MeV}$ electrons, a maximum of $\sim 1.4 \times 10^{16}$ ergs is deposited between 50 km and 30 km altitude and a maximum of $\sim 1.8 \times 10^{16}$ ergs is deposited below 30 km altitude.

This energy deposition is higher than those of Cosmic Rays or Solar Flare particles because of the high RED flux in a limited region of space.

Can the energy deposited in the mesosphere between 50 and ~80 km altitude be important?

we take a 100 km x 100 km x 5 km volume

+6 K temperature increase if the energy is evenly distributed throughout the volume. Clearly “hot spots” will give substantially higher temperatures. Could this directly drive planetary and gravity waves?

NO_x Production, ozone depletion: Tropopause Instability?

With a reduction of ozone in the stratosphere, the solar radiation will be absorbed at the tropopause. **Could the additional heating lead to instability of this structure?**

HCS crossings and atmospheric winds

- *Wilcox et al.* [1973] have reported a relationship between interplanetary heliospheric current sheet (HCS) crossings and atmospheric winds. They studied the average area of high positive vorticity centers (low pressure troughs) observed during northern hemispheric winters at the ~ 300 mbar level.
- Our hypothesis is that it is the REDs associated with the HPS crossings and not the HCS crossings that are causing the Wilcox et al. effect.

HCS crossings, interplanetary relativistic electrons and the global electric circuit

- *Tinsley and Deen* [1991] have proposed that an induced change in the current density of the global electric circuit could lead to climate change. The above paper was related to ionization effects from cosmic rays in the middle stratosphere. Later *Tinsley et al.* [1994] suggested that relativistic solar flare electrons could also cause the same effect.
- In the present paper we find no such interplanetary relativistic electrons, but we do show the disappearance (and suggested precipitation) of relativistic magnetospheric electrons. These magnetospheric particles will have higher energy flux deposition than either cosmic rays or solar relativistic electrons.

We think this is an interesting topic for young researchers in space physics to pursue.

Thank You For Your Attention